High-power single-mode vertical-cavity surface-emitting lasers

N. Samal, S. R. Johnson, D. Ding, A. K. Samal, S.-Q. Yu, and Y.-H. Zhang

Citation: Applied Physics Letters **87**, 161108 (2005); doi: 10.1063/1.2112204
View online: http://dx.doi.org/10.1063/1.2112204
View Table of Contents: http://scitation.aip.org/content/aip/journal/apl/87/16?ver=pdfcov
Published by the AIP Publishing

High-power single-mode vertical-cavity surface-emitting lasers

N. Samal, S. R. Johnson, D. Ding, A. K. Samal, S.-Q. Yu, and Y.-H. Zhang[a)]
Center for Solid State Electronics Research and Department of Electrical Engineering, Arizona State University, Tempe, Arizona 85287-6206

(Received 16 March 2005; accepted 30 August 2005; published online 13 October 2005)

This letter reports a design for high-power single-mode operation in vertical-cavity surface-emitting lasers by means of modal gain control using two different sized current apertures to shape the injection-current profile. A smaller current aperture is located several mirror-pairs away from the active region in the *p*-mirror and a larger current aperture is located in the first *n*-mirror-pair next to the active region. Both theoretical modeling and experimental test results show substantial improvement in the optical mode behavior using this approach when compared to a traditional single-aperture design. A clear trend of the spectral purity in the modal behavior under continuous wave and pulsed conditions is demonstrated and is in good agreement with theoretical predictions. The best design tested demonstrated a room-temperature continuous wave power output of 7.5 mW with a side mode suppression ratio of 20 dB. © *2005 American Institute of Physics*.
[DOI: 10.1063/1.2112204]

Applications for single-mode vertical-cavity surface-emitting lasers (VCSELs) include optical storage, optical interconnects, and laser printing. Furthermore, VCSELs have the potential to replace distributed feedback lasers in optical communication systems provided high-power single-mode operation can be achieved. To date, many approaches to high-power single-mode operation have been reported, such as, cavity spacer layers,[1] shallow surface relief,[2] photonic crystals[3] on the top distributed Bragg reflector (DBR), and antiresonant reflecting optical waveguide[4] structures. This letter reports an alternate approach that utilizes a gain-guided structure with a tailored injection current profile to improve the fundamental mode power output in VCSELs.

A typical way to increase the power output of VCSELs is to increase the area of the active region. This, however, does not favor single fundamental mode operation due to a ring-shaped nonuniform injection-current profile that results from current crowding at edges of the current aperture. Such a carrier distribution[5,6] will result in a gain profile that supports higher-order-mode operation. To solve this inherent problem, we propose an approach that uses different sized current apertures placed on both sides of, and at different distances away from, the active region. This arrangement gives rise to a bell-shaped gain profile that couples well to the fundamental mode of the optical field. The smaller aperture is placed far away from the active region in the *p*-mirror to facilitate current profiling, and the larger aperture is placed near to the active region in the *n*-mirror to facilitate current confinement. The relative size and location of the apertures, as well as the doping profile in the mirrors, governs the spatial profile of injection current in the active region. Three VCSEL designs are considered in this work: two utilizing the alternate design and one utilizing a conventional single-aperture design[7] for comparison. In both alternate designs, the *n*-aperture is approximately twice the diameter of the *p*-aperture and is located in the first mirror-pair of the *n*-DBR. In the first design (design A), the *p*-aperture is placed in the fifth mirror-pair of the *p*-DBR and in the second design (design B), the *p*-aperture is placed in the seventh mirror-pair of the *p*-DBR. In the conventional design (design C) a single oxide aperture is placed in the first mirror-pair of the *p*-DBR. The relative sizes of the apertures and their distances from the active region in the respective designs are shown in Table I for comparison. The modal behavior of designs A and B is compared with the conventional design C using both theoretical modeling and fabricated device results.

The carrier distribution and optical mode are calculated using a two-dimensional spatiotemporal model[8,9] based on laser rate equations that take into account spatial hole burning, carrier diffusion, spontaneous recombination, and the azimuthal dependence of spatially dependent variables such as current spreading, carrier distribution, and transverse modal fields. Instead of using an assumed current injection profile[8,9] the three-dimensional (3D) current injection profile is simulated by solving Poisson's equation using a 3D finite element method, taking into account the doping profile and anisotropic DBR conductivity. To minimize the computation time, the space and time coordinates are separated by modeling the carrier-density profile as a Bessel series expansion.[10] The modal transverse distributions are also calculated in advance by considering the VCSEL cavity as a weakly guiding cylindrical waveguide.[8–11] The time-dependent equations are then solved with a finite difference algorithm. For simplicity, higher-order effects, such as the change in refractive index due to cavity temperature and car-

TABLE I. Comparison of different designs.

		p-aperture		*n*-aperture	
Design	Number of oxide apertures	Distance from active region (μm)	Typical diameter (μm)	Distance from active region (μm)	Typical diameter (μm)
A	2	0.8	14	0.2	24
B	2	1.1	15	0.2	25
C	1	0.2	20	···	···

[a)]Author to whom correspondence should be addressed; electronic mail: yhzhang@asu.edu

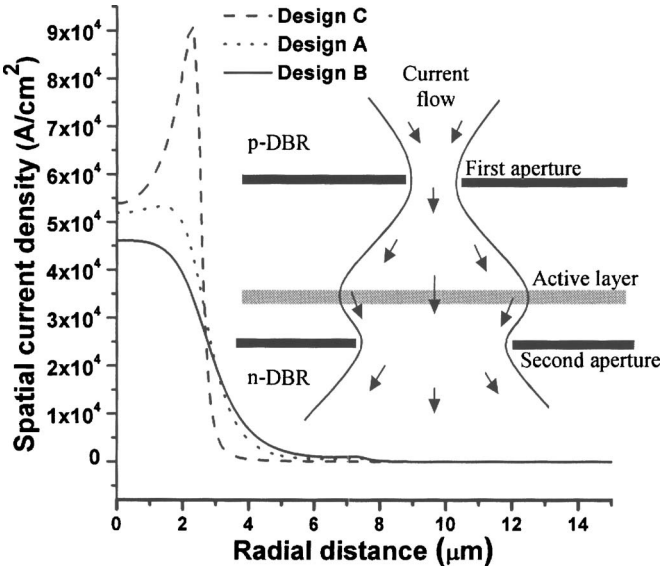

FIG. 1. Simulation results of the spatial current distribution in the active region of VCSELs with various double-current-aperture configurations. The inset shows a schematic cross section of the apertures and current flow.

rier injection, are not taken into account in the present study. For a circularly symmetric oxide VCSEL, the change of refractive index in the active region is a combined effect of the lateral change in the effective refractive index due to the oxide layers, thermal lensing effect, and carrier-induced index changes.[12,13]

The simulation results for the spatial injection-current profile and the carrier-density profile for the three designs are shown in Figs. 1 and 2, respectively; design A is given by the dotted line, design B by the solid line, and design C by the dashed line. The spatial current-density distribution for the conventional VCSEL (design C) shows a distinct ring-shaped injection profile with a maximum at the periphery and a minimum at the center of the device.[5,6] Design A shows a major improvement in the profile. As the *p*-aperture is moved further away from the active region in design B, the spatial current-density profile reaches a favorable bell shape. The inset in Fig. 1 shows a schematic cross section of the double-aperture design. The dominant optical modes for each of the three designs are calculated based on the carrier-density profiles and are shown as insets in Fig. 2. Design C (the upper inset) exhibits many higher-order modes where LP31 is the dominant mode, and the fundamental LP01 mode is more than 40 dB lower in peak intensity. On the other hand, designs A and B (the middle and lower insets, respectively) show that the LP01 mode is dominant, with the next higher mode more than 40 dB lower in intensity for both cases.

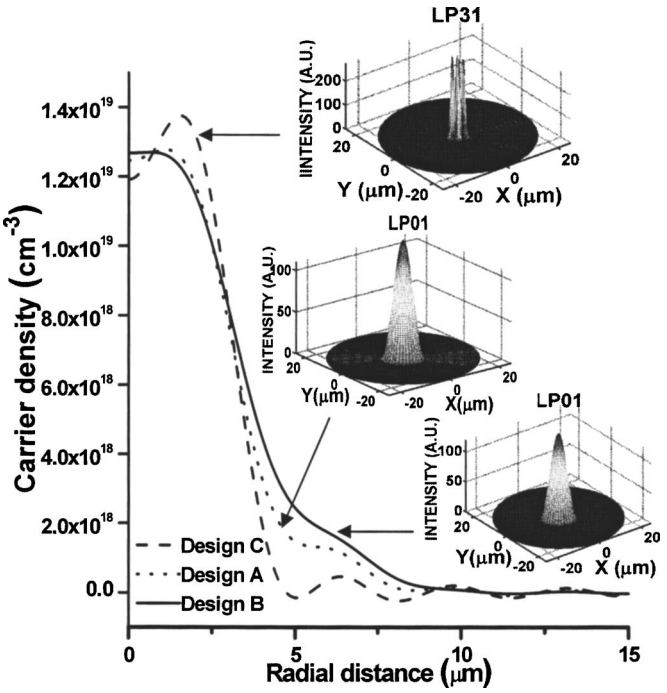

FIG. 2. Simulation results of the carrier-density profiles for three different VCSEL designs. The insets show the dominant transverse optical modes for each design.

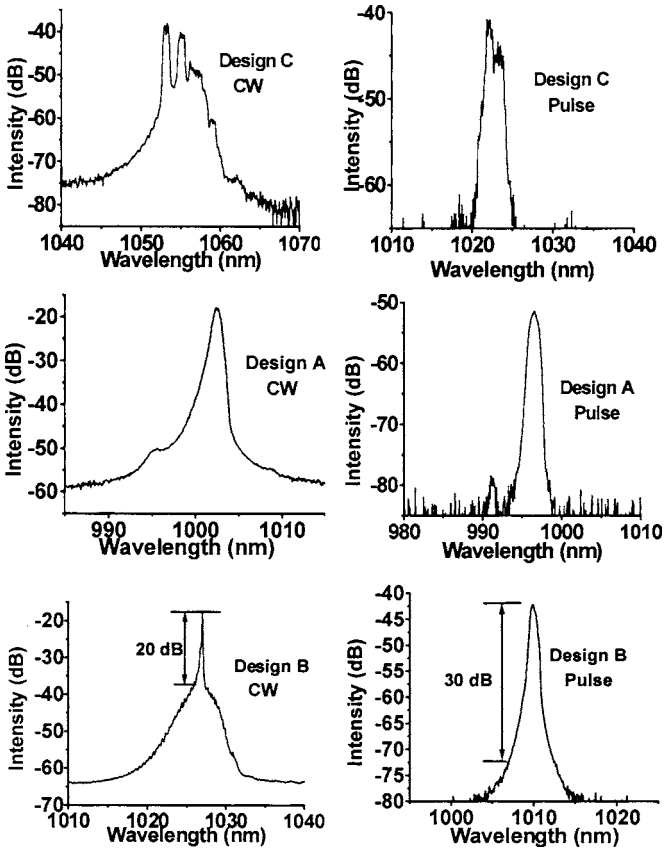

FIG. 3. Cw and pulsed lasing spectra from three different VCSEL designs at a current injection that is three times the threshold. The active regions of these devices are approximately 20 μm in diameter.

Three 1050 nm InGaAs VCSEL wafers (one for each design) were grown using molecular beam epitaxy, and devices with approximately 20 μm diameter active regions (*n*-apertures) were fabricated using a standard wet oxidation VCSEL process. Spectra from a typical device of each design are shown in Fig. 3 under cw and pulsed operation using a 500 ns pulse width and a 1% duty cycle. The cw measurements were taken at an injection current three times the threshold, which corresponds roughly to an injection level that results in a peak cw power output. The pulsed measurements were taken under the same injection level as the cw measurements and serve to identify differences in the spectral performance under a reduced thermal load. A clear trend in spectral purity improvement is observed when going from design C to design B to design A, for both cw and pulsed operation.

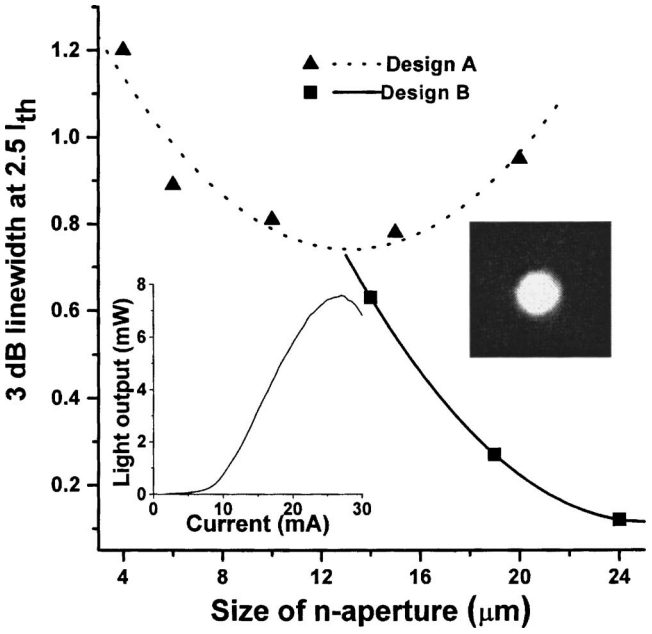

FIG. 4. Spectral linewidth vs *n*-aperture size for VCSEL designs A and B. The left inset shows the cw light output versus current for design B and the right inset shows a near-field image at peak power for design B.

Of all the designs, design B demonstrated the highest power output with the best mode characteristics, achieving a cw power of 7.5 mW with a 3 dB line width of 0.12 nm and a side mode suppression ratio (SMSR) of 20 dB. Power versus injection current for this device is shown in the left inset of Fig. 4; the right inset shows the near-field image. The scatter plots in Fig. 4 show the dependence of the 3 dB line width versus current aperture size for design A (solid triangle with broken line) and design B (solid square with solid line). In each case, the *n*-aperture diameter is given on the *x*-axis and the *p*-aperture diameter is roughly half that of the *n*-aperture. In terms of linewidth, there is an optimum aperture size for each design; the linewidth has a minimum for a 14 μm diameter *n*-aperture in design A and a 24 μm diameter *n*-aperture in design B. These double-aperture structures are inherently gain-guided, since the current apertures do not contribute significantly to index-guiding due to the fact that the *p*-aperture is sufficiently far away from the cavity and the *n*-aperture is sufficiently large.

Under pulse conditions, some cw single-mode VCSELs have been reported to behave as multimode devices.[14,15] Thermal lensing and thermal redistribution of carriers in the active region are thought to be the main contribution to the single-mode operation under cw conditions. In contrast, regardless of pulsed or cw operation, the mode selection in our design is primarily established by the gain profile, which is determined by the double-aperture design. As a result, the pulsed lasing spectra in Fig. 3 show the same trend as the cw spectra, where the spectral purity and SMSR improve from design C to design A to design B. Under pulsed operation, design B exhibits more than 30 dB SMSR. This confirms that neither thermal waveguiding nor the thermal redistribution of carriers determines the modal selection at high injection in these devices. The key to our design is that the shape of the gain profile selects which lateral mode is preferentially excited, and therefore the ability to shape the injection-current profile plays an important role in the mode selection under both cw and pulsed operation.

In conclusion, by using double oxide apertures, gain-guided VCSEL structures for high-power single-mode operation are demonstrated. These designs utilize different sized current confinement apertures at different locations in the DBR mirrors to shape the gain profile. The optical mode behavior of these devices is determined to be superior to that of a traditional single-aperture device using numerical analysis and fabricated devices results. The best design tested demonstrated a room-temperature cw single-mode power output of 7.5 mW with a side mode suppression ratio of 20 dB (30 dB under pulsed conditions).

[1]H. J. Unold, S. W. Z. Mahmoud, R. Jager, M. Kicherer, M. C. Riedl, and K. J. Ebeling, IEEE Photonics Technol. Lett. **12**, 939 (2000).
[2]A. Haglund, J. S. Gustavsson, J. Vukusic, P. Modh, and A. Larsson, IEEE Photonics Technol. Lett. **16**, 368 (2004).
[3]D.-S. Song, S.-H. Kim, H.-G. Park, C.-K. Kim, and Y.-H. Lee, Appl. Phys. Lett. **80**, 3901 (2002).
[4]D. Zhou and L. J. Mawst, IEEE J. Quantum Electron. **38**, 1599 (2002).
[5]C. Degen, W. Elsaber, and I. Fischer, Opt. Express **5**, 37 (1999).
[6]W. Nakwaski, Appl. Phys. A: Mater. Sci. Process. **61**, 123 (1995).
[7]B. Weigl, M. Grabherr, C. Jung, R. Jager, G. Reiner, R. Michalzik, D. Sowada, and K. J. Ebeling, IEEE J. Sel. Top. Quantum Electron. **3**, 409 (1997).
[8]M. X. Jungo, D. Erni, and W. Bächtold, IEEE J. Sel. Top. Quantum Electron. **9**, 939 (2003).
[9]P. V. Mena, J. J. Morikuni, S.-M. Kang, A. V. Harton, and K. W. Wyatt, J. Lightwave Technol. **17**, 2612 (1999).
[10]J. Dellunde, M. C. Torrent, J. M. Sancho, and K. A. Shore, IEEE J. Quantum Electron. **33**, 1197 (1997).
[11]G. R. Hadley, Opt. Lett. **20**, 1483 (1995).
[12]M. Brunner, K. Gulden, R. Hovel, and M. Moser, Appl. Phys. Lett. **76**, 7 (2000).
[13]Y.-G. Zhao and G. McInerney, IEEE J. Quantum Electron. **32**, 1950 (1996).
[14]H. J. Unold, S. W. Z. Mahmoud, R. Jager, R. Michalzik, and K. J. Ebeling, IEEE J. Sel. Top. Quantum Electron. **7**, 386 (2001).
[15]E. W. Young, K. D. Choquette, S. L. Chuang, K. M. Geib, A. J. Fischer, and A. A. Allerman, IEEE Photonics Technol. Lett. **13**, 927 (2001).